

# Modeling L-Dopa Purification by Chiral Ligand-Exchange Chromatography

Nooshafarin Sanaie and Charles A. Haynes

Michael Smith Laboratories and Department of Chemical and Biological Engineering, University of British Columbia, Vancouver, BC, V6T 1Z4, Canada

DOI 10.1002/aic.11111

Published online February 2, 2007 in Wiley InterScience (www.interscience.wiley.com).

*A model describing elution-band profiles that combines multiple chemical equilibria theory with the nonideal equilibrium–dispersion equation for solute transport is used to predict and characterize the separation of L,D-dopa by chiral ligand-exchange chromatography (CLEC). Formation constants and stoichiometries for all equilibrium complexes formed in the interstitial volume and pore liquid are taken from standard thermodynamic databases and independent potentiometric titration experiments. Formation constants for complexes formed with the stationary phase ligand (N-octyl-3-octylthio-D-valine) are determined from potentiometric titration data for a water-soluble analogue of the ligand. This set of pure thermodynamic parameters is used to calculate the spatially discretized composition of each column volume element as a function of time. The model includes a temperature-dependent pure-component parameter, determined by regression to a single elution band for the pure component, that corrects for subtle effects associated with immobilizing the N-octyl-3-octylthio-D-valine ligand onto the stationary phase. The model is shown to accurately predict elution chromatograms and separation performance as a function of key column operating variables. The model is then used to better understand the connection between chemical equilibria within the system and changes in band profiles and band separation resulting from changes in column operating conditions. © 2007 American Institute of Chemical Engineers AIChE J, 53: 617–626, 2007*

**Keywords:** enantiomer separation, dihydroxyphenylalanine, dopa, chemical equilibria

## Introduction

Parkinson's disease is a progressive neurological disorder characterized by akinesia and resting tremor, abnormal posture, bradykinesia, and abnormal rigidity. In advanced stages of the disease, the patient may also experience severe autonomic and sensorimotor dysfunction, cognitive decline, and depression. The predominant pathology of Parkinson's disease is a significant loss of dopaminergic neurons in the substantia nigra. In most instances, the formation of intracellular proteinaceous inclusions throughout the brain is also

observed.<sup>1</sup> The loss of dopaminergic cells results in a reduction in the level of the essential neurotransmitter dopamine. This leads to a progressive reduction of cortical motor output and the associated changes in posture and movement symptomatic of Parkinson's disease.<sup>2,3</sup> In the early stages of Parkinson's disease, normal motor function can be restored by dopamine replacement therapy using the dopamine precursor L-dopa [3-(3',4'-dihydroxyphenyl)-L-alanine] in conjunction with a peripheral dopa-decarboxylase inhibitor (such as benzerazide and carbidopa).

L-Dopa is prepared either by direct enantioselective synthesis or by achiral synthesis of the dopa racemate and separation of the two enantiomers using an appropriate mode of chiral chromatography such as chiral ligand-exchange chromatography (CLEC).<sup>4</sup> Introduced by Davankov and coworkers,<sup>5</sup> CLEC is

Correspondence concerning this article should be addressed to C. Haynes at israelis@chml.ubc.ca.

based on the formation of labile ternary metal complexes, usually at the surface of the stationary phase, between a stereoselective ligand, a transition metal (usually  $\text{Cu}^{2+}$ ), and one of the enantiomers. Resolution of enantiomers is achieved through a small difference in the stabilities of the two diastereomeric ternary complexes, permitting CLEC to be used to separate racemates of amino acids and their derivatives, as well as many important classes of alkaloids, barbiturates,  $\beta$ -blockers, and other adrenergic drugs.<sup>6,7</sup> CLEC separation of racemates generally depends on a complex set of chemical equilibria within the mobile and stationary phases of the column. As a result, the separation efficiency (resolution) profoundly depends on a number of column operating variables, including temperature, pH, ligand density, and the concentrations of the enantiomers and the transition metal in the feed. Although identification of suitable operating conditions for separation of enantiomers by CLEC can be achieved through proper design of experiments, we recently showed that process optimization can be achieved more rapidly and exhaustively using a new model for enantiomer transport and elution that combines the classic reaction-diffusion theory of chromatography with multiple chemical equilibria theory. The latter theory is used to define all chemical speciation and adsorption equilibria within the column.<sup>8</sup>

In this work, we apply our model to prediction of elution chromatograms for the separation of an l,d-dopa racemate by CLEC. Because of its 3',4'-dihydroxyphenyl side chain, dopa possesses a large number of protonation states and  $\text{Cu}^{2+}$  binding sites (Figure 1). The chemical equilibria driving the CLEC-based separation of dopa enantiomers are therefore unusually complex, making modeling of this process particularly challenging. Performance of the model in predicting elution chromatograms and separation performance as a function of key column operating variables is reported. The model is then used to better understand the connection between chemical equilibria within the system and changes in band profiles and peak separation resulting from changes in column operating conditions.

## Theory

### Model development

The complete derivation of our model is provided elsewhere<sup>8</sup> and we thus present here only its key features. The structure of the model is based on results from first- and second-moment analysis of experimental elution chromatograms that confirm that solute mass transfer within the column is limited by the rate of diffusion within the pores of the stationary phase. As a result, the condition of local equilibrium can be assumed at all times at every radial position within the spherical stationary-phase particle. Multiple chemical equilibria theory is used to calculate the concentration of each diastereomeric ternary complex formed at the stationary-phase surface along with the chemical speciation profiles

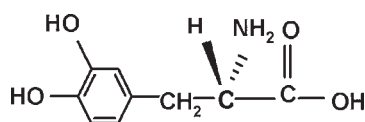


**Figure 1. Structure of l-dopa: 3-(3',4'-dihydroxyphenyl)-l-alanine.**

within the mobile phase and pore liquid. Speciation is used here in the usual thermodynamic sense and refers to the complete set of equilibrium components and complexes present in the system. For a cylindrical column of length  $L$  packed with a stationary phase composed of spherical sorbent particles of radius  $R_p$  and porosity  $\varepsilon_p$ , the continuity equation for mass transport of any solute  $i$  within the interstitial volume of void fraction  $\varepsilon$  is given by

$$\frac{\partial c_i}{\partial t} = D_L \frac{\partial^2 c_i}{\partial z^2} - \frac{u}{\varepsilon} \frac{\partial c_i}{\partial z} - \frac{(1-\varepsilon)}{\varepsilon} \frac{\partial s_i}{\partial t} \quad (1)$$

where  $c_i(z, t)$  (mol/m<sup>3</sup> bulk fluid) is the total concentration of component  $i$  in the mobile phase (assumed to be independent of the radial and angular position within the column cross section),  $D_L$  is the axial dispersion coefficient (m<sup>2</sup> s<sup>-1</sup>),  $u$  is the superficial liquid velocity (m s<sup>-1</sup>), and  $z$  is the axial position coordinate. The total concentration  $c_i$  of component  $i$  includes the moles of free component  $i$  in the mobile phase plus the moles of  $i$  in all complexes present in the mobile phase. The average solute concentration  $s_i(z, t)$  (mol/m<sup>3</sup> adsorbent particle) within the stationary-phase particles located at column position  $z$  is given by

$$s_i(z, t) = \frac{\int_0^{R_p} [\varepsilon_p c_i^*(r, z, t) + (1-\varepsilon_p) q_i^*(r, z, t)] 4\pi r^2 dr}{\frac{4}{3}\pi R_p^3} \quad (2)$$

where  $c_i^*(r, z, t)$  (mol/m<sup>3</sup> pore fluid) and  $q_i^*(r, z, t)$  (mol/m<sup>3</sup> adsorbent particle) are the total concentration of the solute in the intraparticle fluid and adsorbed to the sorbent surface, respectively.

Solution of the continuity equation requires knowledge of the rate of solute uptake  $\partial s_i / \partial t$  within the porous sorbent particles, given by

$$\frac{(1-\varepsilon)}{\varepsilon} \frac{\partial s_i}{\partial t} = \frac{3(1-\varepsilon)}{R_p \varepsilon} D_p \left( \frac{\partial c_i^*}{\partial r} \right)_{r=R_p} \quad (3)$$

where  $D_p$  is the intraparticle diffusivity of the solute (m<sup>2</sup> s<sup>-1</sup>).

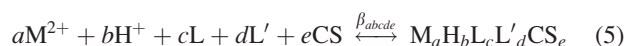
Finally, gradients in free solute concentration within the pores of the stationary phase are determined through a corresponding solute mass balance within the bead

$$\frac{\partial c_i^*}{\partial t} = D_p \left( \frac{\partial^2 c_i^*}{\partial r^2} + \frac{2}{r} \frac{\partial c_i^*}{\partial r} \right) - \frac{1-\varepsilon_p}{\varepsilon_p} \frac{\partial q_i^*}{\partial t} \quad (4)$$

Solution of Eq. 4 requires a model for chemical equilibria relating  $q_i^*(r, z, t)$  to the chemical speciation of component  $i$  in the adjacent pore fluid.

### Determination of chemical equilibria

Chemical speciation in chiral ligand-exchange chromatography systems is governed by a set of equilibrium formation reactions of the general form



where  $\text{M}^{2+}$  is the metal ion (that is,  $\text{Cu}^{2+}$ ),  $\text{H}^+$  is the proton,  $\text{L}$  is the fully deprotonated (free) l-enantiomer,  $\text{L}'$  is the fully

deprotonated d-enantiomer, CS is the fully deprotonated chiral selector (*N*-octyl-3-octylthio-d-valine, a derivative of d-penicillamine, in this application), and *a*–*e* represent the stoichiometric coefficients for the equilibrium complex. The formation constant  $\beta_{abcde}$  is defined in terms of equilibrium concentrations of the reactants. We therefore designate  $\beta_{abcde}$  as a concentration formation constant to clearly differentiate it from a formation constant based on the activities of the reactants. It is important to recognize that the major thermodynamic databases for bidentate ligand complexes almost exclusively report concentration formation constants because activity coefficients for the pure and complexed components are rarely available.<sup>9,10</sup> Thus, in many cases, the required  $\beta_{abcde}$  values can be taken from the literature and need not be measured. A negative value for the stoichiometric coefficient *b* indicates the presence and number of hydroxyl ions in the complex.

In our model, equilibria equations (Eq. 5) are combined with total mass balance equations for  $M^{2+}$ ,  $H^+$ ,  $L$ ,  $L'$ , and CS to obtain a set of nonlinear algebraic equations that may be solved to determine the equilibrium composition at any solution temperature and pH. For example, the total mass balance for the metal ion is given by

$$T_M = [M^{2+}] + \sum_k a_k [M_{a_k} H_{b_k} L_{c_k} L'_{d_k} CS_{e_k}]$$

$$= [M^{2+}] + \sum_k a_k \beta_{a_k, b_k, c_k, d_k} [M^{2+}]^{a_k} [H^+]^{b_k} [L]^{c_k} [L']^{d_k} [CS]^{e_k} \quad (6)$$

where  $T_M$  represents the total concentration of the metal ion (mol/L) in the system and  $\beta_{a_k, b_k, c_k, d_k, e_k}$  is the formation constant for complex *k*. With all model parameters known, including the equilibrium formation constant for each complex present, Eqs. 1–6 can be solved to predict composition profiles within and exiting the column as a function of time. Boundary conditions and a description of the Crank–Nicolson scheme<sup>11</sup> used to approximate differentials by a central difference in time and an average central difference in space are described in detail elsewhere.<sup>8</sup> The column was meshed in the *z* dimension to match or exceed the number of theoretical units (NTUs) within the column and the number of radial volume elements within the stationary-phase particle was set equal to 5.

## Experimental

### Materials and methods

Dopa enantiomers, copper sulfate ( $CuSO_4$ ) pentahydrate, potassium nitrate ( $KNO_3$ ), and copper nitrate [ $Cu(NO_3)_2$ ] were purchased from Sigma–Aldrich Chemical Canada Ltd. (Oakville, Ontario, Canada). The chemicals were always of the highest available purity (>99%) and were used without further purification. The d-penicillamine derivative (*p*-methylbenzyl-d-penicillamine) used as a solution-phase analogue of the chiral selector was purchased from Peptides International Inc. (Louisville, KY). Water used in all experiments was first distilled and then treated with a NANOpure® II ultrafiltration system (Barnstead, Dubuque, IA). All solutions for the HPLC system were filtered through 0.22  $\mu m$  (GV) Durapore filters (Millipore, Bedford, MA) and degassed before use. The Waters HPLC system (Waters, Milford,

MA) used in these studies consists of a 717 autosampler, a 486 UV detector, a 410 differential refractor, and a 600S controller. A 610 Waters column heater was used to control the column and preheat the feed to the desired operating temperature.

### Potentiometric titrations

Protonation constants for l,d-dopa and formation constants for all complexes formed between l-dopa, d-dopa, and the  $Cu^{2+}$  ion were determined by potentiometric titration for two solvent systems: water and an aqueous solution containing 10% isopropanol. Details of the potentiometric titration protocol were described previously.<sup>12</sup> Potentiometric titrations were also used to determine protonation constants for the chiral selector, as well as formation constants for binary complexes formed between  $Cu^{2+}$  and the chiral selector and for ternary CS,  $Cu^{2+}$ , and l,d-dopa mixed-ligand complexes. In these experiments, a water-soluble analogue (*p*-methylbenzyl-d-penicillamine, hereafter referred to as *p*-MBD-penicillamine) of the chiral selector (*N*-octyl-3-octylthio-d-valine) was used to allow titrations to be conducted in a single phase. The sulfide-protecting methylbenzyl group was included in the analogue to prevent disulfide bond formation, which leads to the reduction of Cu(II) to Cu(I) through donation of an electron to copper. Equilibrium formation constants were regressed from potentiometric titration data using the chemometric program *Chemeq* described previously.<sup>13</sup>

### Chromatography experiments

CLEC studies were performed on a Chirex 3126 column from Phenomenex Inc. (Torrance, CA). The stationary phase consists of porous silica particles with an average particle diameter of 5  $\mu m$  and an average pore diameter of 110 Å. The particles are packed into a stainless steel column of length *L* = 150 mm and inner diameter 4.6 mm. The *N*-octyl-3-octylthio-d-valine chiral selector is physically immobilized on the silica matrix through hydrophobic interactions between its dioctyl tail and the C18 brush grafted onto the silica matrix (Figure 2). The column manufacturer reports the density of the chiral selector immobilized on the Chirex 3126 column to be 50 mM.

Degassed stock solutions (90% water, 10% isopropanol) of each enantiomer (10 mM l- or d-dopa) were made in 2 mM  $CuSO_4$  such that the  $[Cu]/[dopa]$  ratio was 1:5. A stock solution of the racemate (10 mM total dopa) was then prepared by

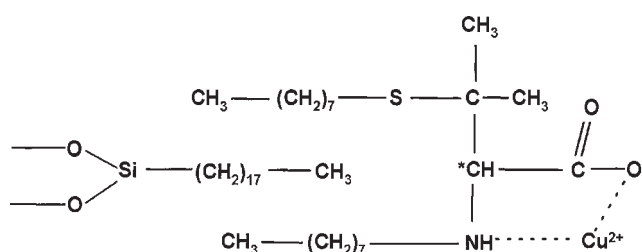


**Figure 2.** Structure of the chiral selector (*N*-octyl-3-octylthio-d-valine) immobilized through hydrophobic bonding with the C18 reversed-phase chemistry of the Chirex 3126 column.

**Table 1. Column Characteristics, Mass Transfer Coefficients, and Some Dimensionless Parameters Characterizing the Transport of L-Dopa Injected onto the Chirex 3126 Column as a 10- $\mu$ L Pulse at a Flow Rate of 1 mL min<sup>-1</sup> at 298.15 K**

Parameter	Symbol (Unit)	Value
Column length	$L$ (m)	0.15
Column radius	$R_c$ (m)	$2.3 \times 10^{-3}$
Bead radius	$R_p$ (m)	$2.5 \times 10^{-6}$
Column void	$\varepsilon$	$0.32 \pm 0.01$
Stationary phase porosity	$\varepsilon_p$	$0.81 \pm 0.01$
Average pore diameter	$P_d$ (m)	$1.1 \times 10^{-8}$
Kinematic viscosity of mobile phase	$\nu$ (m <sup>2</sup> /s)	$9.09 \times 10^{-7}$
Column axial dispersion coefficient	$D_L$ (m <sup>2</sup> /s)	$5.8 \pm 0.2 \times 10^{-8}$
Overall mass transfer coefficient	$K_m$ (s <sup>-1</sup> )	$14.07 \pm 0.35$
Pore diffusion coefficient	$D_p$ (m <sup>2</sup> /s)	$6.15 \pm 0.2 \times 10^{-12}$
Film mass transfer coefficient	$k_f$ (m/s)	$9.05 \pm 0.1 \times 10^{-4}$
Interstitial velocity	$u_0$ (m/s)	$3.14 \times 10^{-3}$
Peclet number	$Pe = Lu/D_L$	$2.60 \pm 0.09 \times 10^3$
Biot number	$Bi = k_f R_p/D_p$	$368 \pm 16$
Forward rate constant	$k_{ads}$ (s <sup>-1</sup> )	$\geq 7.60 \times 10^4$
Damköhler number	$Da = k_{ads} R_p^2/D_p$	$\geq 7.72 \times 10^4$
Reynolds number	$Re = 2R_p u/\nu$	$5.5 \times 10^{-3}$

mixing equal volumes of each enantiomer stock solution. All samples were filtered through a Gelman<sup>®</sup> Acrodisc 0.2- $\mu$ m PVDF (polyvinylidene fluoride) syringe filter (Pall Gelman Sciences Corp., Ann Arbor, MI) before injection into the column. Experiments were performed at a volumetric flow rate of 1 mL/min. The column was equilibrated with at least 10 column volumes of mobile phase (90% water, 10% isopropanol) before each 10- $\mu$ L sample injection. Eluent from the column was monitored by UV absorbance at 254 nm.

## Results and Discussion

### Column properties and solute transport characteristics

Table 1 reports the geometric properties of the Chirex 3126 column as well as mass transfer coefficients and related parameters describing the transport of (l,d)-dopa within the mobile and stationary phases of the column. The first- and second-moment analysis method of Ruthven<sup>14</sup> was applied to determine the fraction of external voids ( $\varepsilon$ ) and all solute transport parameters inside the column by analyzing inlet and elution peak shapes as a function of interstitial velocity.<sup>15–17</sup> Details of the linear velocity range and tracer molecules used are provided by Sanaie and Haynes.<sup>8</sup> Results from this analysis were used to compute dimensionless groups that allowed determination of the rate-limiting resistance to solute mass transfer within the column. Both the Damköhler number ( $Da > 10^4$ ) and the Biot number ( $Bi \simeq 370$ ) are large, indicating that solute diffusion through the pores of the stationary phase limits the overall rate of adsorption to the porous resin. This permits the local equilibrium approximation to be applied throughout the column (that is,  $q_i$  can be computed from the equilibrium adsorption isotherm equation, derived below using multiple chemical equilibria theory, everywhere in the column).

### Equilibrium formation constants for the Cu<sup>2+</sup>-dopa-*p*-MBD-penicillamine system

The multiple chemical equilibria theory encoded in our CLEC model requires a set of equilibrium formation constants and reaction stoichiometric coefficients for complexes formed within the mobile and stationary phases of the CLEC column. The speciation in aqueous systems containing protons, a transition metal ion, and a catecholamine such as dopa can be quite complex, necessitating a careful set of potentiometric and spectroscopic studies to identify the dopa-Cu<sup>2+</sup> species formed and to determine all related thermodynamic parameters.<sup>18,19</sup>

**Protonation Constants.** Dopa [3-(3',4'-dihydroxyphenyl)-alanine] is a polyprotic acid for which it can be difficult to assign measured protonation constants to specific functional groups arising from overlap of protonation states. This problem is generally overcome by defining a set of “macro”-protonation constants that define the overall protonation state of the compound but are not linked to specific titratable groups. Jameson<sup>20</sup> used linear free-energy relations and kinetic evidence in an attempt to assign the order of protonation of dopa, which begins with either one of the phenolato groups of the catechol ring, and proceeds with protonation of the second phenolato group, the  $\alpha$ -amino group, and finally the  $\alpha$ -carboxyl group. However, the protonation states of the phenolato groups and the  $\alpha$ -amino group are partially overlapping, making it difficult to precisely assign the second and third protonation states of dopa.

Measured equilibrium formation constants for all H<sup>+</sup>-dopa species are reported in Table 2. All are in good agreement with previous studies, confirming the accuracy of the proton titration experiments carried out in this work.<sup>19,21</sup> The four stepwise macroprotonation constants ( $pK_a$ ) of dopa may be computed from the reported  $\beta$  values by subtracting  $\beta_{0j100}$  from  $\beta_{0(j+1)100}$ ; the  $pK_a$  value for species 04100 of dopa in aqueous solution is therefore 2.20. Although the effect is small, the addition of 10% isopropanol increases the two highest macro-protonation constants ( $pK_a$  for species 01100 and  $pK_a$  for species 02100), which we believe correspond to the two phenolato groups on the catechol, and also increases the  $pK_a$  for species 04100, which can be unambiguously assigned to the  $\alpha$ -carboxyl group.

**Table 2. Protonation Constants for Dopa or *p*-MBD-penicillamine Determined from Potentiometric Titration Experiments in Two Different Solvent Systems: Water and an Aqueous Solution Containing 10% Isopropanol**

System	Log <sub>10</sub>	Aqueous	90% Water, 10% Isopropanol
Cu <sup>2+</sup> , H <sup>+</sup> , L-dopa,	$\beta_{01100}^*$	$13.3 \pm 0.1^\dagger$	$13.4 \pm 0.4$
D-dopa,	$\beta_{02100}$	$23.18 \pm 0.04$	$23.5 \pm 0.2$
<i>p</i> -MBD-	$\beta_{03100}$	$31.95 \pm 0.02$	$31.8 \pm 0.2$
penicillamine	$\beta_{04100}$	$34.15 \pm 0.03$	$34.1 \pm 0.2$
	$\beta_{01001}$	$8.51 \pm 0.02$	$8.42 \pm 0.03$
	$\beta_{02001}$	$10.4 \pm 0.1$	$10.5 \pm 0.1$

Note:  $T = 298.15$  K,  $I_c = 0.1$  M KNO<sub>3</sub>.

\*The subscript “*abcde*” on  $\beta_{abcde}$  indicates the molecules of Cu<sup>2+</sup> (a), protons (b), L-dopa (c), D-dopa (d), and chiral selector analogue (*p*-MBD-penicillamine) (e) present in complex *abcde*.

<sup>†</sup>Errors reported as the standard deviation from the mean for 10 to 15 independently regressed data sets.



Addition of 10% isopropanol decreases the  $pK_a$  of species 03100, which strongly suggests that this  $pK_a$  represents the protonation constant for the  $\alpha$ -amino group. Addition of an organic alcohol to the mobile phase lowers the dielectric constant of the solvent and therefore increases electrostatic forces between charged groups. Thus, the activity of the proton is increased in the presence of isopropanol, shifting mass action away from the free proton and toward neutral complexes containing the proton. Thus, the  $pK_a$  values for the two phenolato groups are expected to increase with addition of isopropanol, as is observed with the  $pK_a$  values of species 01100 and 02100, whereas the  $pK_a$  value for the  $\alpha$ -amino group is predicted to decrease, as is observed for species 03100. In a recent study<sup>17</sup> we observed similar trends for  $\alpha$ -amino acid protonation constants when methanol served as the organic cosolvent.

Aqueous-phase protonation constants for the chiral selector analogue (*p*-MBD-penicillamine) are similar but not identical to those reported previously for the carboxylic (the  $pK_a$  for species 02001 is reported to be 1.91<sup>22,23</sup>) and  $\alpha$ -amino ( $pK_a$  for species 01001 reported to be 8.10<sup>23</sup>) groups of penicillamine. The addition of 10% isopropanol decreases the  $pK_a$  for species 01001, the protonation constant for the  $\alpha$ -amino group, and increases the  $pK_a$  for the  $\alpha$ -carboxyl group. As with dopa, the addition of organic cosolvent therefore disfavors the zwitterionic state of *p*-MBD-penicillamine in favor of the neutral forms of each titratable group on the molecule.<sup>17,24,25</sup>

**Equilibrium Formation Constants for Binary and Ternary Complexes.** Equilibrium speciation in aqueous solutions containing dopa and transition metals has been the subject of intense study because of its biological importance.<sup>18,19,21</sup> In the presence of a transition metal ion, dopa can form a traditional amino-acid type O,N bidentate complex with  $\text{Cu}^{2+}$  by its  $\alpha$ -carboxyl and  $\alpha$ -amino groups, and pyrocatechol type O,O bidentate complexes by its two phenolato groups. UV and ESR (electronic spin resonance) spectral studies by Gergely and Kiss<sup>19</sup> of the copper (II)/d,l-dopa system indicate that at low pH (<5) amino acid-type complexes of composition  $\text{CuH}_2\text{A}$  and  $\text{Cu}(\text{H}_2\text{A})_2$  are preferentially formed, whereas at higher pH values (>9) the pyrocatechol-type complex  $\text{Cu}(\text{HA})_2$  and its various deprotonated species are favored. In the intermediate pH range ( $5 < \text{pH} < 9$ ), amino

acid-type complexes are favored, but cyclic and open-chain dimeric species are also produced in appreciable amounts, including complexes containing both N,O and O,O bonds.

Speciation within the  $\text{Cu}^{2+}$ - $\text{H}^+$ -dopa system is also strongly dependent on the  $\text{Cu}^{2+}$  to dopa ratio. As a result, determination of formation constants for all  $\text{Cu}^{2+}$ - $\text{H}^+$ -dopa complexes formed in solution is not possible in a single titration experiment and, instead, requires regression of titration data recorded at two or more metal-ligand ratios. When the  $\text{Cu}^{2+}$  to dopa ratio is 1 to 1, standard 1:1 and 1:2 amino-acid type complexes are favored, although significant amounts of dimetallic complexes ( $\text{Cu}_2\text{H}_2\text{A}_2$  and  $\text{Cu}_2\text{A}_2$ ) can also form, particularly at higher pH, as a result of dopa behaving as a bridging ligand. When the  $\text{Cu}^{2+}$  to dopa ratio is 1 to 2, formation of dimetallic complexes is significantly reduced, permitting more accurate regression of formation constants for those complexes containing a single  $\text{Cu}^{2+}$  ion.<sup>26-28</sup>

Equilibrium formation constants for binary  $\text{Cu}^{2+}$ -( $\text{H}^+$ )-dopa complexes and binary  $\text{Cu}^{2+}$ -*p*-MBD-penicillamine complexes formed in water and in aqueous solutions containing 10% isopropanol are reported in Table 3. Together, the formation constants indicate that the addition of 10% isopropanol shifts equilibria toward formation of *bis* binary complexes, thereby reducing the concentration of uncomplexed dopa and *p*-MBD-penicillamine in the system, particularly at solution pH values > 3.5. The stability of the *mono* binary  $\text{Cu}^{2+}$ -*p*-MBD-penicillamine complex, the active form of the chiral selector, also increases appreciably.

The overall equilibrium formation constant for the dominant ternary complexes (species 12101 and 12011) also increases with addition of isopropanol (Table 4). Stabilization of these neutral ternary complexes occurs not only because of the lower dielectric permittivity of the cosolvent, but also through the lower hydrogen bonding potential of isopropanol, which disfavors solvation of Cu(II) through coordination of the oxygen of isopropanol to one of the four planar or two distal coordination sites of the metal ion. As a result, the displacement of an alcohol ligand by a dopa enantiomer or the chiral selector is favored relative to the displacement of a water molecule complexed with the metal ion.

**Species Distribution within the Chirex CLEC Column.** Our potentiometric titration data show that up to 30 species can

**Table 3. Equilibrium Formation Constants for Binary  $\text{Cu}^{2+}$ -( $\text{H}^+$ )-L-Dopa or  $\text{Cu}^{2+}$ -*p*-MBD-penicillamine Complexes Determined from Potentiometric Titration Data in Two Different Solvents: Water and an Aqueous Solution Containing 10% Isopropanol**

System	Log <sub>10</sub>	Aqueous	90% Water, 10% Isopropanol	[L-dopa]:[Cu]
$\text{Cu}^{2+}$ , $\text{H}^+$ , L-dopa	$\beta_{14200}$	$60.4 \pm 0.3^\dagger$	$60.5 \pm 0.2$	1:1
	$\beta_{13200}$	$54.1 \pm 0.4$	$53.5 \pm 0.3$	2:1
	$\beta_{12200}$	$45.3 \pm 0.4$	$45.5 \pm 0.1$	2:1
	$\beta_{11200}$	$35.4 \pm 0.3$	$36.2 \pm 0.1$	2:1
	$\beta_{10200}$	$25.3 \pm 0.3$	$25.8 \pm 0.1$	2:1
	$\beta_{12100}$	$30.6 \pm 0.1$	$30.7 \pm 0.1$	1:1
	$\beta_{22200}$	$53.1 \pm 0.2$	$53.4 \pm 0.2$	1:1
	$\beta_{20200}$	$41.9 \pm 0.2$	$42.4 \pm 0.1$	1:1
	$\beta_{10001}$	$7.35 \pm 0.11$	$7.49 \pm 0.04$	2:1
$\text{Cu}^{2+}$ , $\text{H}^+$ , <i>p</i> -MBD-penicillamine	$\beta_{10002}$	$14.64 \pm 0.09$	$14.67 \pm 0.08$	2:1

Note:  $T = 298.15 \text{ K}$ ,  $I_c = 0.1 \text{ M KNO}_3$ .

\*The solution concentration of L-dopa to Cu(II) used in the titration experiment is also reported in the fifth column. The titration experiments covered a pH range from 3 to 6.5 when the L-dopa to  $\text{Cu}^{2+}$  ratio was 1:1 and from 6.5 to 11.5 when the ratio was 2:1. The last two entries in the fifth column indicate the solution concentration ratio of *p*-MBD-penicillamine to Cu(II) used in the titration experiment.

†Errors reported as the standard deviation from the mean for 10 to 15 independently regressed data sets.

**Table 4. Ternary Equilibrium Formation Constants for  $\text{Cu}^{2+}$  · L-Dopa · *p*-MBD-penicillamine or  $\text{Cu}^{2+}$  · D-Dopa · *p*-MBD-penicillamine Complexes Determined from Potentiometric Titration Measurements in Two Different Solvents: Water and an Aqueous Solution Containing 10% Isopropanol\***

System	Log <sub>10</sub>	Aqueous	90% Water, 10% Isopropanol	$k_f$
Cu, H, L-dopa, <i>p</i> -MBD-penicillamine	$\beta_{12101}$	$37.6 \pm 0.2^\dagger$	$37.9 \pm 0.5$	$2.1 \times 10^{-2}$
	$\beta_{11101}$	$31.8 \pm 0.5$	$31.7 \pm 0.7$	—
Cu, H, D-dopa, <i>p</i> -MBD-penicillamine	$\beta_{12011}$	$37.1 \pm 0.3$	$37.6 \pm 0.4$	$3.2 \times 10^{-2}$
	$\beta_{11011}$	$31.6 \pm 0.4$	$31.9 \pm 0.5$	—

Note:  $T = 298.15 \text{ K}$ ,  $I_c = 0.1 \text{ M KNO}_3$ .

\*The on-column correction factor  $k_f$  is also reported.

<sup>†</sup>Errors reported as the standard deviation from the mean for 10 to 15 independently regressed data sets.

form within the mobile and stationary phases of the Chirex CLEC column during the separation of l,d-dopa. However, differences in the magnitudes of the formation constants reported in Tables 2–4 indicate that not all of these complexes will be present in the column under normal column operating conditions. The manufacturer recommends operating the Chirex 3126 column at 2 mM  $\text{Cu}^{2+}$  with 10 mM racemate in the feed pulse. The operating pH is typically set between 3.5 and 6, with a value between 5 and 5.5 being the most common. Consider then the injection of only l-dopa onto the column under this range of recommended operating conditions. The resulting dominant chemical equilibria are shown in Figure 3, which reports the solution of Eq. 6 within a central volume element of the l-dopa elution band when the Chirex column is operated at 25°C with a 10% isopropanol/90% water mobile phase containing 2 mM  $\text{CuSO}_4$ . Although more than two dozen equilibrium complexes are formed under these conditions, only species 04100, 03100, 12101, 11101, 14200, 22200, 12100, 10001, and 01001 are present at significant concentrations. Moreover, at pH values  $\leq 5.5$ , the concentration of the 12101 ternary complex is much higher than that of the 11101 complex. We have used this knowledge to simplify the model by including in our multiple chemical equilibria equations only those complexes (04100, 03100, 12101, 14200, 22200, 12100, 10001, 01001, and the corresponding complexes for d-dopa) that are present at sufficiently high concentrations to influence the elution behavior of the enantiomers.

### Modeling the separation of dopa enantiomers

The formation constant data reported in Tables 2–4 suggest that it should be possible to use *p*-MBD-penicillamine to separate l,d-dopa racemates in water. However, the Chirex 3126 column cannot be operated in pure water because the chiral selector (*N*-octyl-3-octylthio-d-valine) is immobilized through hydrophobic bonding of the dioctyl tail with the C18 chemistry of the underlying resin. As with all reverse-phase columns, the structure of the C18 brush is sensitive to solvent polarity and collapses in pure water, effectively eliminating proper column function. As a result, all elution chromatograms and modeling results refer to a mobile phase containing 10% isopropanol.

Although the  $\beta_{12101}$  and  $\beta_{12011}$  values reported in Table 4 define the stabilities of the two ternary mixed-ligand complexes in solution, they do not account for changes in complex stabilities arising from minor differences in the chemis-

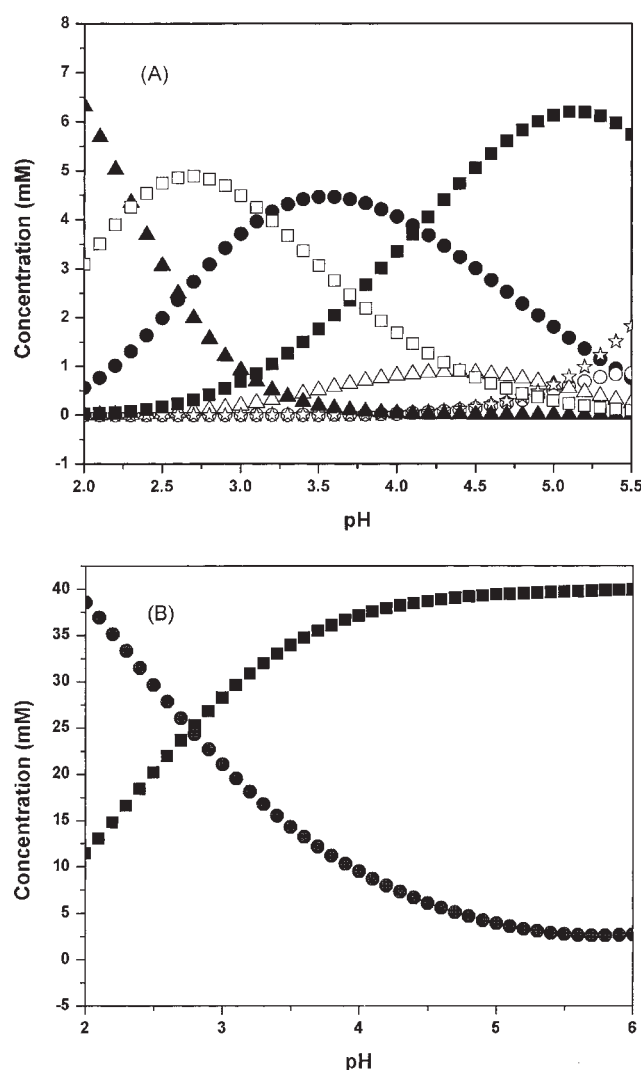


**Figure 3. pH dependency of major complexes formed in an aqueous solution containing 10% isopropanol, 2 mM  $\text{CuSO}_4$ , and 10 mM l-dopa injected as a 10- $\mu\text{L}$  pulse onto the Chirex 3126 column at 1 mL min<sup>-1</sup>.**

The column was maintained at 298.15 K and contained 50 mM immobilized *N*-octyl-3-octylthio-d-valine. (A) Open squares: complex 03100; filled triangles: 04100; filled squares: 12101; open stars: 11101; open triangles: 14200; open circles: 22200; and filled circles: 12100. (B) Filled squares: 10001; and filled circles: 01001.

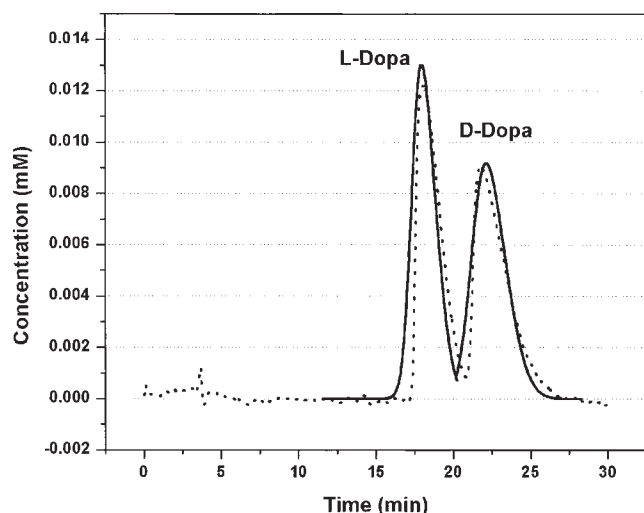


**Figure 4. Comparison between experimental (dashed line) and model (solid line) elution profiles for a 10- $\mu$ L pulse injection of 10 mM d,l-dopa onto the Chirex 3126 column.**

The aqueous mobile phase (1 mL min<sup>-1</sup>) contained 10% isopropanol and 3 mM CuSO<sub>4</sub> at pH 5.4. The column was maintained at 298.15 K and contained 50 mM immobilized *N*-octyl-3-octylthio-d-valine.

try of the chiral selector (*N*-octyl-3-octylthio-d-valine) relative to that of the solution-phase analogue (*p*-MBD-penicillamine) used in the titration studies. Nor do they include the effect (such as steric packing changes and the like) of immobilizing the chiral selector onto the surface of the stationary phase. Although generally quite small, these effects influence CLEC elution band profiles in subtle ways<sup>8</sup> that can be accounted for by defining a constant  $k_l$

$$\log(\beta_{ijklm}^*) = (1 + k_l) \log(\beta_{ijklm}) \quad (7)$$

that may be used to determine the on-column ternary formation constant  $\beta_{ijklm}^*$  from the corresponding value  $\beta_{ijklm}$  for the solution-phase analogue. Reported in Table 4,  $k_l$  values were determined by model regression to the elution band profiles for a 10- $\mu$ L pulse injection of each pure enantiomer (10 mM) onto the Chirex column operating at a flow rate of 1 mL min<sup>-1</sup> and a mobile phase pH and CuSO<sub>4</sub> concentration of 5.4 and 2 mM, respectively. Each  $k_l$  value is a function of temperature only. For both enantiomers,  $k_l$  is quite small, providing no more than a 3% correction to the value of  $\beta_{ijklm}$ . As a result, the elution behavior of dopa enantiomers on the Chirex column can be described with reasonable accuracy using tabulated formation constants obtained from standard thermodynamic databases, provided an appropriate solution-phase analogue of the chiral selector can be identified. However, precise modeling of the chromatographic behavior requires inclusion of the small correction factor  $k_l$ .

Figure 4 compares with experiment the predicted chromatogram for a 10- $\mu$ L pulse injection of a 10-mM dopa racemate onto the Chirex 3126 column at a flow rate of 1 mL min<sup>-1</sup>, a temperature of 25°C, and a mobile phase pH of 5.4. Unlike the conditions used to regress  $k_l$ , the mobile-phase Cu<sup>2+</sup> concentration is now 3 mM. The model accurately pre-

dicts the experimental chromatogram. Similar agreement is observed at other operating conditions (see below), indicating that the model can be used to map the l,d-dopa separation efficiency as a function of column operating conditions.

**Copper Concentration Effects.** Mobile-phase copper concentration is known to have a profound influence on the quality of CLEC-based separations.<sup>8,29–32</sup> For the Chirex column operated at pH 5.4, Figure 5 reports experimental retention times for both l- and d-dopa as a function of Cu<sup>2+</sup> concentration under otherwise constant column operating conditions. An increase in [Cu<sup>2+</sup>] results in a nonlinear decrease in the retention times of both enantiomers, with the decrease in the retention of the more retained enantiomer being considerably more pronounced. Model analysis reveals that the observed decrease in retention time with increasing [Cu<sup>2+</sup>] results from changes in chemical equilibria that reduce partitioning of the enantiomer into the stationary phase. This can be seen in Figure 6, which compares chemical equilibria within a central volume element of the elution band for l-dopa when the Chirex column is operated at two different mobile-phase Cu<sup>2+</sup> concentrations: 1 mM CuSO<sub>4</sub> and 3 mM CuSO<sub>4</sub>. Only those complexes present at concentrations large enough to influence the elution behavior of the enantiomer are shown. At pH 5.4 (the mobile phase pH used to collect the data shown in Figure 5), an increase in the Cu<sup>2+</sup> concentration increases the concentration of activated chiral selector (species 10001) (Figure 6b), but also shifts chemical equilibria in the mobile phase toward Cu(II)-containing l-dopa complexes (Figure 6a). Formation of the dominant ternary complex (species 12101) at the stationary phase then requires release of a Cu<sup>2+</sup> ion into the solution phase.

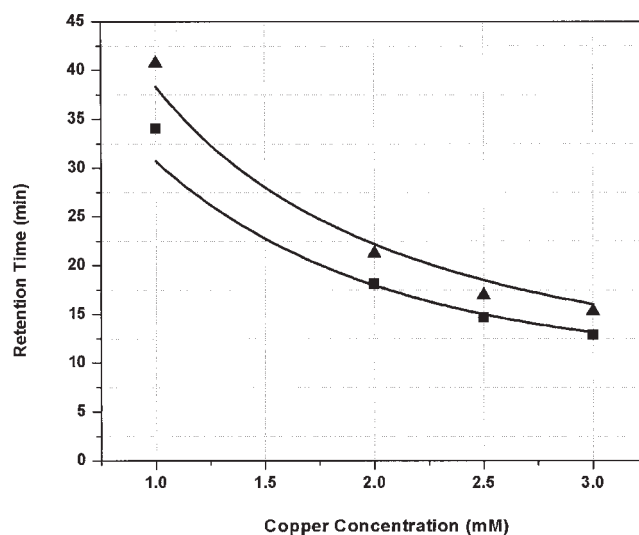


**Figure 5. Comparison as a function of mobile-phase Cu(II) concentration between experimental (filled squares: l-dopa; filled triangles: d-dopa) and predicted (solid lines) retention times for dopa enantiomers (10 mM d,l-dopa) injected as a 10- $\mu$ L pulse onto the Chirex 3126 column at 1 mL min<sup>-1</sup>.**

The column was maintained at 298.15 K and contained 50 mM immobilized *N*-octyl-3-octylthio-d-valine. The mobile phase contained 10% isopropanol at pH 5.4.

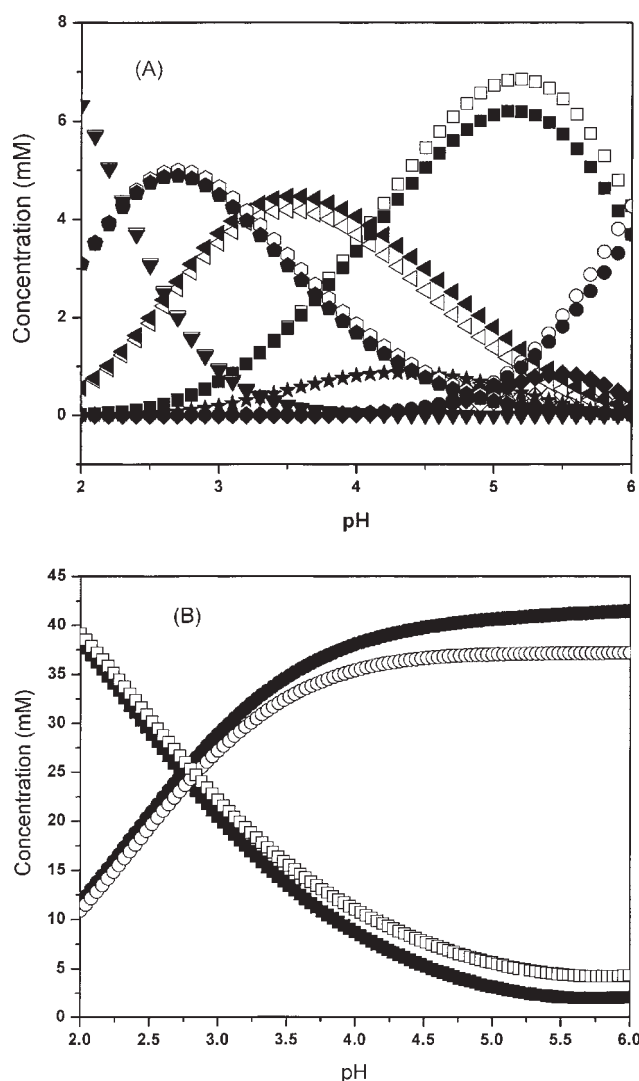
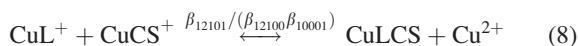


**Figure 6. pH dependency of the dominant equilibrium complexes in an aqueous mixture at 298.15 K containing 10 mM l-dopa, 50 mM *N*-octyl-3-octylthio-d-valine, and 10% isopropanol.**

The copper concentration in the system was set at 47.24 mM, corresponding to the total concentration of Cu(II) when the mobile phase Cu(II) concentration is 1 mM, or at 51.68 mM, the total Cu(II) when the mobile phase Cu(II) concentration is 3 mM. The open and filled symbols represent complexes when [Cu(II)] is 1 and 3 mM, respectively, in the mobile phase. (A) Squares: complex 12101; circles: 11101; stars: 14200; diamonds: 22200; triangles: 12100; inverse triangles: 04100; pentagons: 03100. (B) Squares: 01001; circles: 10001.



which is thermodynamically disfavored at high  $\text{Cu}^{2+}$  concentrations. As a result, although it increases the density of active stationary-phase ligand, an increase in  $\text{Cu}^{2+}$  in the mobile phase reduces formation of the ternary complex, leading to the observed decrease in enantiomer retention time.

The quality of a chromatographic separation is often measured by the resolution  $R_s$ , which is equal to the ratio of the

distance between the peak maxima to the mean band width of the two neighboring peaks,  $\bar{w}$ :

$$R_s = \frac{\Delta t_R}{\bar{w}} = \frac{2(t_{R,2} - t_{R,1})}{(w_1 + w_2)} \quad (9)$$

where  $t_{R,1}$  and  $t_{R,2}$  are the retention times of components 1 and 2, and  $w_1$  and  $w_2$  are the peak widths measured by the baseline intercept. As shown in Figure 7, model predictions accurately capture the complex dependency of the resolution on  $\text{Cu}^{2+}$  concentration.

**pH Effects.** Figure 8 compares with experiment predicted retention times for l- and d-dopa as a function of pH. As is generally observed in CLEC separations<sup>33–35</sup> the retention times of both enantiomers decrease nonlinearly with decreasing pH, with the retention time for the d-enantiomer showing a more pronounced decline. At  $\text{pH} \leq 3.2$ , the retention times for the two enantiomers become identical and equal to the elution time of the column void; no separation is predicted or observed at these pH values.

Predictions of the dependency of the resolution ( $R_s$ ) on pH agree well with experiment (Figure 9), indicating that our model is capable of quantitatively capturing the dependency of the separation performance on primary column operating parameters. It also allows us to understand the underlying molecular phenomena through analysis of changes in the distribution of various complexes in the system after a change in operating conditions (such as pH,  $\text{Cu}^{2+}$  concentration,  $[\text{Cu}^{2+}]/[\text{dopa}]$ , and so forth). For example, in the pH range of 4 to 5.5, increasing the pH results in a corresponding increase in the concentration of the activated chiral selector (species 10001) and a concomitant decrease in the protonated state of the chiral selector (species 01001) (Figure 3b). Simi-

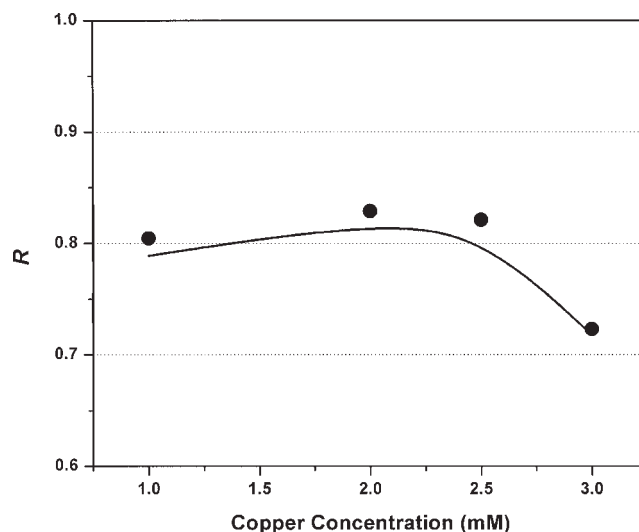


**Figure 7. Comparison between the experimental (filled circles) and predicted (solid lines) resolution of dopa enantiomers as a function of mobile phase Cu(II) concentration.**

The data apply to a 10- $\mu\text{L}$  pulse of 10 mM l,d-dopa injected onto the Chirex 3126 column at a flow rate of 1  $\text{mL min}^{-1}$ . The column was maintained at 298.15 K and contained 50 mM immobilized *N*-octyl-3-octylthio-d-valine. The mobile-phase contained 10% isopropanol at pH 5.4.



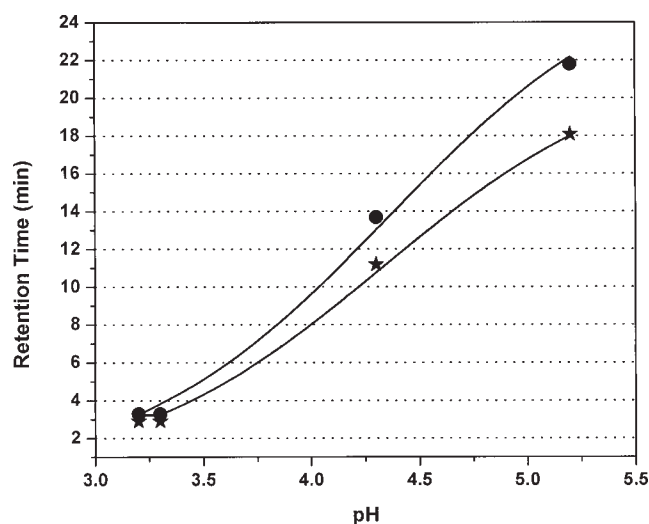


**Figure 8. Dependency of retention time on pH.**

Comparison between experimental (l-dopa: filled stars; d-dopa: filled circles) and predicted (line) retention times for injection of 10 mM d,l-dopa as a 10- $\mu$ L pulse onto the Chirex 3126 column operated at 298.15 K. The column contained 50 mM *N*-octyl-3-octylthio-d-valine. The aqueous mobile phase contained 10% isopropanol and 2 mM  $\text{CuSO}_4$ . The flow rate was 1 mL  $\text{min}^{-1}$ .

larly, the concentrations of various protonated forms of the two enantiomers to be separated diminish with increasing pH, thereby avoiding the thermodynamically unfavorable release of free protons into a proton-rich solution during ternary complex formation. In contrast, at low pH the free enantiomers mainly exist in two highly protonated states, species 03100 and 04100. Formation of a ternary complex then must proceed by a reaction between fully or highly pro-

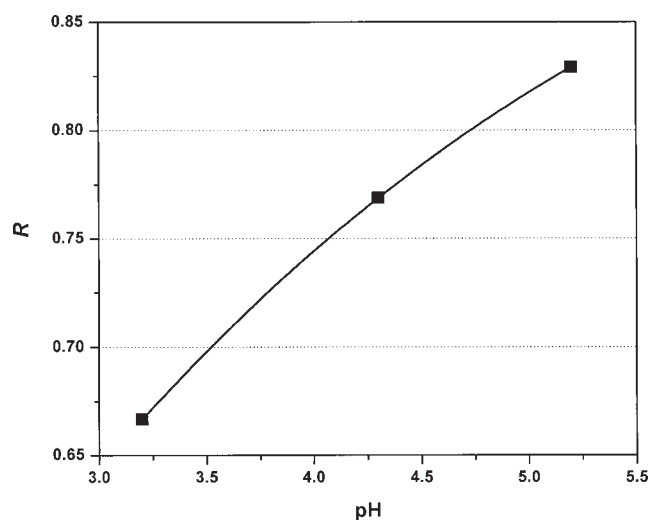


**Figure 9. Comparison between experimental (filled squares) and model (solid line) results for the resolution *R* of dopa enantiomers on the Chirex 3126 column.**

A 10- $\mu$ L pulse of 10 mM l,d-dopa was injected onto the column (298.15 K) at a flow rate of 1 mL  $\text{min}^{-1}$ . The aqueous mobile phase contained 10% isopropanol and 2 mM  $\text{CuSO}_4$ .

tonated forms of the enantiomer and the chiral selector, resulting in a sharp decrease in the concentration of the dominant ternary complexes (12101 and 12011). Finally, because the stability of the hetero-chiral l-dopa- $\text{Cu}^{2+}$ -chiral selector complex is less than that of the homo-chiral d-dopa- $\text{Cu}^{2+}$ -chiral selector complex, the model predicts a stronger impact of the mobile phase pH on the retention time of the d-enantiomer, as observed experimentally (Figure 8).

## Conclusions

l-Dopa has served as a primary treatment of Parkinson's disease for over 30 years. We have shown that the separation behavior of a dopa racemate within the *N*-octyl-3-octylthio-d-valine-bearing CLEC column can be accurately predicted by incorporating a complete description of solution and surface chemical equilibria into a traditional one-dimensional reaction-diffusion model of chromatography. The model relies on a set of equilibrium formation constants and reaction stoichiometries that can be taken from standard thermodynamic databases or measured to a high degree of accuracy through regression of potentiometric titration data. Although fairly difficult to solve because of the complex speciation within the system, the model quantitatively captures the dependency of the elution chromatogram on key column operating variables, thereby providing a facile route to interpret the mechanism of separation and to determine optimum column operating conditions.

## Acknowledgments

This work was funded by grants from Pfizer Corp. and the Natural Sciences and Engineering Research Council of Canada (NSERC). NS is the recipient of a University Graduate fellowship from NSERC. CAH holds the Canada Research Chair in Interfacial Biotechnology and is partially funded by the National Research Council of Canada.

## Literature Cited

- Zhang J, Goodlett DR, Quinn JF, Peskind E, Kaye JA, Zhou Y, Pan C, Yi E, Eng J, Wang Q, Aebersold RH, Montine TJ. Quantitative proteomics of cerebrospinal fluid from patients with Alzheimer disease. *J Alzheimers Dis.* 2005;7:125–133.
- Schultz W. Getting formal with dopamine and reward. *Neuron.* 2002;36:241–263.
- Fearnley JM, Lees AJ. Striatonigral degeneration. A clinicopathological study. *Brain.* 1990;113:1823–1842.
- Husain S, Sekar R, Rao RN. Enantiomeric separation and determination of antiparkinsonian drugs by reversed-phase ligand-exchange high-performance liquid chromatography. *J Chromatogr A.* 1994;687:351–355.
- Davankov VA, Rogozhin SV. Ligand chromatography as a novel method for the investigation of mixed complexes: Stereoselective effects in amino acid-copper(II) complexes. *J Chromatogr.* 1971;60:280–283.
- Brückner H, Bosch I, Graser T, Fürst P. Determination of alpha-alkyl-alpha-amino acids and alpha-amino alcohols by chiral-phase capillary gas-chromatography and reversed-phase high-performance liquid-chromatography. *J Chromatogr.* 1987;395:569–590.
- Galli B, Gasparrini F, Misiti D, Villani C, Corradini R, Dossena A, Marchelli R. Enantiomeric separation of dansyl-amino and dansylamino acids by ligand-exchange chromatography with (S)-phenylalaninamide-modified and (R)-phenylalaninamide-modified silica-gel. *J Chromatogr A.* 1994;666:77–89.
- Sanaie N, Haynes CA. A multiple chemical equilibria approach to modeling and interpretation of the separation of amino acid enan-

- tiomers by chiral ligand-exchange chromatography. *J Chromatogr A*. 2006;1132(1-2):39–50.
9. Martell AE, Smith RM. Critically selected stability constants of metal complexes. *The National Institute of Standards and Technology (NIST). Standard Reference Database 46*, Version 6.0. Gaithersburg, MD: NIST; 2001.
  10. Pettit LD, Powell KJ. *The IUPAC Stability Constants Database (SC-Database)*. Otley, UK: Academic Software/International Union of Pure and Applied Chemistry; 2003.
  11. Crank J, Nicolson P. A practical method for numerical evaluation of partial differential equations of the heat conduction type. *Proc Comb Philos Soc* 1947;43:50–67.
  12. Sanaie N, Haynes CA. Formation constants and coordination thermodynamics for binary and ternary complexes of copper(II), L-hydroxyproline, and an amino acid enantiomer. *J Chem Eng Data*. 2005;50:1848–1856.
  13. Koska J, Mui C, Haynes CA. Solvent effects in chiral ligand exchange systems. *Chem Eng Sci*. 2001;56:29–41.
  14. Ruthven DM. *Principles of Adsorption and Adsorption Processes*. New York: Wiley; 1984.
  15. Guiochon G, Shirazi SG, Katti AM. *Fundamentals of Preparative and Nonlinear Chromatography*. Boston, MA: Academic Press; 1994.
  16. Ladisch MR. *Bioseparations Engineering: Principles, Practice, and Economics*. New York: Wiley; 2001.
  17. Sanaie N, Haynes CA. Interpreting the effects of temperature and solvent composition on separation of amino-acid racemates by chiral ligand-exchange chromatography. *J Chromatogr A*. 2006;1104:164–172.
  18. Patel P, Bhattacharya PK. Study of formation and stability of binary and ternary binuclear Cu(II) complexes involving L-dopa. *J Inorg Biochem*. 1994;53:57–68.
  19. Gergely A, Kiss T. Complexes of 3,4-dihydroxyphenyl derivatives. 1. Copper(II) complexes of dl-3,4-dihydroxyphenylalanine. *Inorg Chim Acta*. 1976;16:51–59.
  20. Jameson RF. Assignment of proton-association constants for 3-(3,4-dihydroxyphenyl)alanine (L-dopa). *J Chem Soc Dalton Trans*. 1978: 43–45.
  21. Kiss T, Gergely A. Complexes of 3,4-dihydroxyphenyl derivatives. 3. Equilibrium study of parent and some mixed-ligand complexes of dopamine, alanine and pyrocatechol with nickel(II), copper(II) and zinc(II) ions. *Inorg Chim Acta*. 1979;36:31–36.
  22. Hynes MJ, O'Dowd M. Interactions of the trimethyltin(IV) cation with carboxylic-acids, amino-acids, and related ligands. *J Chem Soc Dalton Trans*. 1987:563–566.
  23. Nair MS, Arasu PT, Pillai MS, Natarajan C. Mixed-ligand complexes involving sulfur-containing ligands. 2. Nickel(II) ternary complexes of L-cysteine, D-penicillamine and L-cysteic acid with imidazoles. *J Chem Soc Dalton Trans*. 1993:917–921.
  24. Shehata MR, Shoukry MM, Barakat MH. Coordination properties of 6-aminopenicillanic acid: Binary and ternary complexes involving biorelevant ligands. *J Coord Chem*. 2004;57:1369–1386.
  25. Köseoglu F, Kilic E, Dogan A. Studies on the protonation constants and solvation of alpha-amino acids in dioxan-water mixtures. *Anal Biochem*. 2000;277:243–246.
  26. Zelano V, Zerbinati O, Ostacoli G. Ternary Cu(II) complex-formation with L-dopa or dopamine and valine, leucine, phenylalanine and threonine in aqueous-solution. *Ann Chim (Rome)*. 1988;78:273–283.
  27. Daniele PG, Ostacoli G, Zerbinati O. Thermodynamic and spectrophotometric study of copper(II) L-dopa complexes in aqueous-solution. *Ann Chim (Rome)*. 1990;80:89–99.
  28. Kiss T, Gergely A. Copper(II) and nickel(II) ternary complexes of L-dopa and related compounds. *J Inorg Biochem*. 1985;25:247–259.
  29. Hyun MH, Han SC, Lee CW, Lee YK. Preparation and application of a new ligand exchange chiral stationary phase for the liquid chromatographic resolution of alpha-amino acid enantiomers. *J Chromatogr A*. 2002;950:55–63.
  30. Hyun MH, Han SC, Whangbo SH. New ligand exchange chiral stationary phase for the liquid chromatographic resolution of alpha- and beta-amino acids. *J Chromatogr A*. 2003;992:47–56.
  31. Zheng ZX, Lin JM, Qu F, Hobo T. Chiral separation with ligand-exchange micellar electrokinetic chromatography using a D-penicillamine-copper(II) ternary complex as chiral selector. *Electrophoresis*. 2003;24:4221–4226.
  32. Doury-Berthod M, Poitrenaud C, Tremillon B. Ligand-exchange separation of amino-acids. 2. Influence of the eluent composition and of the nature of the ion-exchanger. *J Chromatogr*. 1979;179:37–61.
  33. Belov YP, Aksinenko AY, Blessington B, Newman AH. Chiral aminophosphonate eluent for enantiomeric analysis of amino acids. *Chirality*. 1996;8:122–125.
  34. Śliwka M, Ślebioda M, Kolodziejczyk AM. Dynamic ligand-exchange chiral stationary phases derived from N-substituted (S)-phenylglycinol selectors. *J Chromatogr A*. 1998;824:7–14.
  35. Galaverna G, Corradini R, Dallavalle F, Folesani G, Dossena A, Marchelli R. Chiral separation of amino acids by copper(II) complexes of tetradentate diaminodiamido-type ligands added to the eluent in reversed-phase high-performance liquid chromatography: A ligand exchange mechanism. *J Chromatogr A*. 2001;922:151–163.

Manuscript received July 7, 2006, and revision received Dec. 12, 2006.